ZIRCON U-PB AGES OF THE VALDEZ GROUP AND THE PASSAGE CANAL AND BILLINGS PLUTONS, FROM THE PASSAGE CANAL AREA OF PRINCE WILLIAM SOUND, ALASKA

Robert J. Gillis, Paul B. O'Sullivan, and Ray A. Donelick

Raw Data File 2024-29

Billings pluton freshly exposed at the toe of the retreating Billings Glacier, Prince William Sound, Alaska

2024
STATE OF ALASKA
DEPARTMENT OF NATURAL RESOURCES
DIVISION OF GEOLOGICAL & GEOPHYSICAL SURVEYS

STATE OF ALASKA
Mike Dunleavy, Governor

DEPARTMENT OF NATURAL RESOURCES
John Boyle, Commissioner

DIVISION OF GEOLOGICAL & GEOPHYSICAL SURVEYS
Melanie Werdon, State Geologist & Director

Publications produced by the Division of Geological & Geophysical Surveys are available to download from the DGGS website (dggs.alaska.gov). Publications on hard-copy or digital media can be examined or purchased in the Fairbanks office:

Alaska Division of Geological & Geophysical Surveys (DGGS)
3354 College Road | Fairbanks, Alaska 99709-3707
Phone: 907.451.5010 | Fax 907.451.5050
dggspubs@alaska.gov | dggs.alaska.gov

DGGS publications are also available at:

Alaska State Library, Historical
Collections & Talking Book Center
395 Whittier Street
Juneau, Alaska 99801

Alaska Resource Library and
Information Services (ARLIS)
3150 C Street, Suite 100
Anchorage, Alaska 99503

Suggested citation:
Gillis, R.J., O'Sullivan, P.B., and Donelick, R.A., 2024, Zircon U-Pb ages of the Valdez Group and the Passage Canal and Billings plutons, from the Passage Canal area of Prince William Sound, Alaska: Alaska Division of Geological & Geophysical Surveys Raw Data File 2024-29, 13 p.
https://doi.org/10.14509/31427

ZIRCON U-PB AGES OF THE VALDEZ GROUP AND THE PASSAGE CANAL AND BILLINGS PLUTONS, FROM THE PASSAGE CANAL AREA OF PRINCE WILLIAM SOUND, ALASKA

Robert J. Gillis[1], Paul B. O'Sullivan[2], and Ray A. Donelick[2]

INTRODUCTION

The zircon U-Pb results provided in this report supplement geologic mapping of the Passage Canal area near Whittier, Alaska, to constrain the ages of major mapped bedrock units (Bull and others, 2024). These include Cretaceous Valdez Group marine strata and the Passage Canal and Billings plutons. Files associated with this publication can be downloaded from doi.org/10.14509/31427.

LIST OF DELIVERABLES

- Methods report
- Summary data spreadsheet and accompanying data dictionary
- Analytical lab data and accompanying data dictionary provided by GeoSep Services

METHODS

Sample Collection

We selected approximately 10–15 kg of the freshest, most unaltered and unweathered rock available at each of three sampled locations. Sample 12BG300A was a medium- to fine-grained sandstone metamorphosed to greenschist facies. Samples 12BG303A and 12BG308A were phaneritic intrusive rocks with unaltered mafic mineral phases, visible striae on crystal faces, and appeared to be free of chloritic alteration or oxidation. Sample locations were recorded using modern, hand-held GPS units set to UTM Zone 6 (NAD27) coordinates with typical horizontal precision of 9 to 21 feet. Locations presented herein were converted to NAD27 geographic coordinates.

Sample preparation

Zircon grains were isolated and prepared for Laser Ablation-Inductively Coupled Plasma-Mass Spectrometry (LA-ICP-MS) analyses. Each sample was crushed using a jaw crusher to <5 mm, and the crushate was sieved using 300-micron nylon mesh. The <300-micron fraction was washed with tap water and dried at room temperature in air, and zircon was isolated using standard gravimetric and magnetic mineral separation techniques. Zircon grains were mounted in epoxide resin and polished to a smooth finish using 0.3-micron alumina slurry. Zircon grain mounts were stirred

[1] Alaska Division of Geological & Geophysical Surveys, 3354 College Road, Fairbanks, AK 99709
[2] GeoSep Services, 1520 Pine Cone Rd., Moscow, ID 83843

vigorously in reagent-grade 5.5 molar nitric acid for 20 seconds at 21°C and rinsed with distilled water to remove any common lead contamination.

LA-ICP-MS Data Collection

Zircon U-Pb data were acquired at Donelick Properties in Viola, Washington, using a Resonetics RESOlution M-50 ArF Excimer 193 nm laser attached to an Agilent 7700x quadrupole inductively coupled plasma mass spectrometer using the following standards:

B2	~1,128 Ma (Donelick and Donelick, written commun.)
B3	~1,128 Ma (Donelick and Donelick, written commun.)
DR	31.44 ± 0.18 Ma (Boyce and Hodges, 2005; McDowell and others, 2005)
FC	1,099.0 ± 0.6 Ma (Paces and Miller, 1993)
F5	1,099.0 ± 0.6 Ma (assumed equal to FC-1) (Paces and Miller, 1993)
IF	28.201 ± 0.012 Ma (Lanphere and Baadsraard, 2001; Kuiper and others, 2008)
MD	99.12 ± 0.14 Ma (Renne and others, 1998)
MM	523.98 ± 0.12 Ma (Schoene and Bowring, 2006)
MT	732 ± 5 Ma (Black and Gulson, 1978; Yuan and others, 2008)
OL	913 ± 7 Ma (Barfod and others, 2005)
S9	1,065.4 ± 0.6 Ma (Yuan and others, 2008; Weidenbeck and others, 1995)
TI	390.5 ± 0.5 Ma (Roden and others, 1990)

LA-ICP-MS Data Modeling

The data for each spot on a single zircon grain were characterized by a series of data scans, each scan representing one measurement for each mass in order of increasing mass. The series of data scans may be divided into background and signal+background segments. Background represents data collected prior to firing the laser. Signal+background represents data collected during laser ablation of the spot.

The following steps were taken to determine background-corrected signal intensities for each mass analyzed for each spot: (1) the true time was calculated over which each measurement was collected for each mass for each scan; the time at which background ends and signal+background begins was determined using selected masses; (2) a line was fitted to all background values for each mass prior to the time at which background ends; (3) outlier background values were removed and the regression repeated. For a negative slope, the background value for the current mass was set equal to the value of the line at the time at which background ends; the error was set equal to the standard deviation of the background values about the fitted line. For zero or positive slope, the background value for the current mass was set equal to the mean of the fitted background values; the error was set equal to the standard deviation of the background values about the mean.

- Signal+background values were smoothed (versus scan number) for each mass using a Savitzky and Golay (1964) filter based on the median of fitted polynomials; the error of each signal+background value was set equal to the standard deviation of the signal+background values about the smoothed curve.
- Background-corrected signal values were calculated by subtracting background from signal+background values. Background-corrected signal error values were calculated using background error and signal+backround error values.

The following steps were taken to calculate isotopic ages and their errors for each spot in a session:

In each primary standard spot, common Pb was assumed negligible, and fractionation factors (accepted isotopic ratio divided by the measured ratio) and their errors were calculated for each scan using background-corrected signal values and their errors (Donelick and others, 2009). Fractionation factors and their errors were smoothed (versus spot number) using a Savitzky and Golay (1964) filter based on the median of fitted polynomials. Fractionation factors and their errors were used by interpolation/extrapolation to calculate ages and their errors for each scan at each spot in the session. Only concordant scans, where all ages overlap at the 2-sigma (σ) error level, were used to calculate weighted-mean isotopic ratios for a spot. Weighted-mean isotopic ratios of concordant scans were used to calculate the isotopic ages for a spot. For all spots in a session, a value proportional to radiation dose (function of calculated isotopic age, uranium, and thorium contents) was calculated. Also, the ratio of accepted isotopic age versus measured isotopic age was calculated for each primary and secondary standard spot. A linear regression was obtained giving isotopic age ratio for the standards versus radiation dose. Ages were again calculated for concordant scans using weighted-mean isotopic ratios corrected for radiation dose (Donelick and others, 2009).

The data were considered concordant if their ratios overlapped concordia within 2σ analytical uncertainty (Spencer and others, 2016). Systematic uncertainties were propagated by quadrature prior to calculation of the weighted mean of all magmatic samples (Horstwood and others, 2016). For determining the maximum depositional date from detrital samples, systematic uncertainties were added by quadrature to the weighted mean of the youngest cluster of grain dates that overlapped within 2σ (Horstwood and others, 2016; Coutts and others, 2019). For this study, all weighted-mean calculations, and weighted mean, Concordia, and kernel density estimate plots were determined and produced using IsoplotR (Vermeesch, 2018).

Maximum depositional ages (MDA) defined by populations of young zircons were determined for the Valdez Group sample. To determine its MDA, we calculated the youngest statistical population (youngest statistical population [YSP]; Coutts and others, 2019; Herriott and others, 2019). This approach is a reliable means of calculating an MDA with a low likelihood of producing a date that is younger than the true stratigraphic age of the sampled interval (Coutts and others, 2019).

Determining the crystallization age of an igneous rock requires dating only zircons that grew immediately prior to magma crystallization (autocrystic grains; Miller and others, 2007). However, igneous rocks can contain significant quantities of antecrystic zircons (older grains that suggest long magma residence times [Hildreth, 2001; Charlier and others, 2005]) and xenocrystic grains inherited from wall rock that must be excluded prior to calculating the weighted mean (WM). Few strategies have been developed for distinguishing antecrystic and xenocrystic grains in LA-ICP-MS data (e.g., Campbell and others, 2006; Seigel and others, 2018), and a standardized approach for doing so has not been established. We, therefore, use the commonly adopted method of calculating the WM of the entire zircon distribution, recognizing that the resulting mean standard weighted deviation (MSWD) is much greater than 1.0 and the probability of fits of zero indicates dispersion of dates greater than expected for a genetically congruent population.

Sample Descriptions

Sample 12BG300A – Valdez Group

Sample12BG300A (Latitude/Longitude: 60.80260/-148.85042) is a fine-upper to medium-lower grain size, moderately sorted sandstone with subrounded to subangular grains. The sample is metamorphosed to greenschist facies and outcrops near minor, medium-bedded slate with possible weak S-C fabric parallel to bedding.

Sample 12BG303A – Passage Canal Pluton

Sample 12BG303A (Latitude/Longitude: 60.86881/-148.49242) is a granite composed of 34 percent granophyric potassium feldspar crystals 3 mm to 1 cm long with Carlsbad twinning and plagioclase inclusions. Quartz crystals 2 mm to 1 cm long constitute 34 percent of the sample with overgrowths on some crystals and tiny unidentified inclusions. Undulose extinction and embayed, cracked quartz crystals are common. The rock consists of 24 percent plagioclase crystals with sericite and lamellar twins, 2 to 4 mm long. Biotite crystals (3 percent) are variably altered to chlorite, and exhibit dark red-brown and light brown pleochroism; some show birds-eye extinction. The sample also contains trace muscovite and opaques (the latter often enclosed within altered biotite).

Sample 12BG308A – Billings Pluton

12BG308A (Latitude/Longitude: 60.85443/-148.59760) is a granite consisting of 34 percent granophyric potassium feldspar crystals 3 mm to 1 cm long with Carlsbad twinning and plagioclase inclusions. Thirty-four percent quartz crystals 2 mm to 1 cm long with overgrowths on some crystals and tiny unidentified inclusions. Common undulose extinction and embayed, cracked crystals. Twenty-four percent plagioclase 2 to 4 mm long, commonly with sericite and lamellar twins. Three to 5 percent biotite, mostly altered to chlorite with dark red-brown and light brown pleochroism; Some birds-eye extinction. Some muscovite and trace opaques (the latter often enclosed within altered biotite). Plagioclase and potassium feldspars exhibit possible perthitic textures.

RESULTS

Sample 12BG300A – Valdez Group: 66.1±1.5 (MSWD=1.01, probability of fit [PoF] =0.36) Maximum Depositional Age

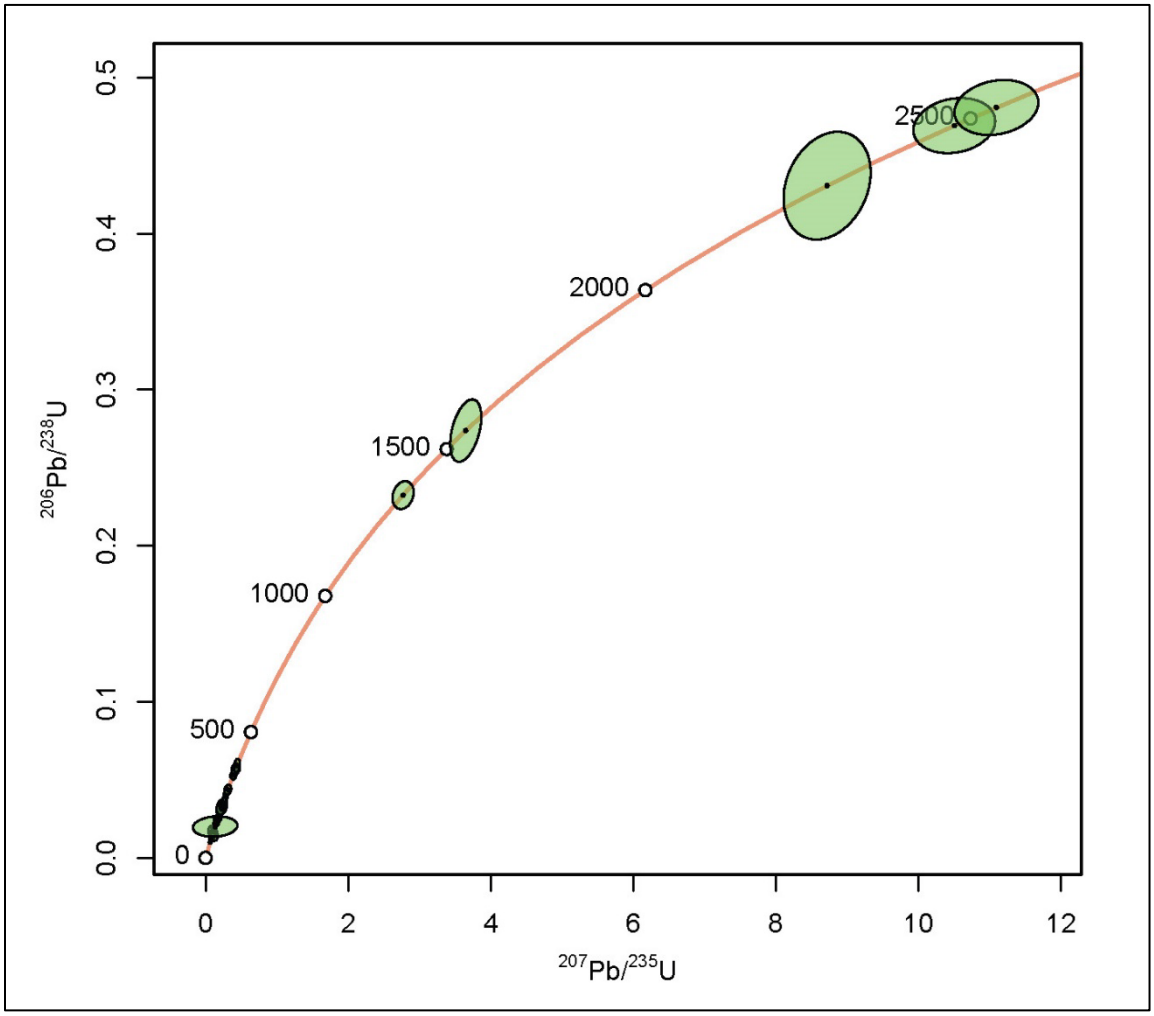

Figure 1. Concordia diagram of individual zircon U-Pb analyses for sample 12BG300A.

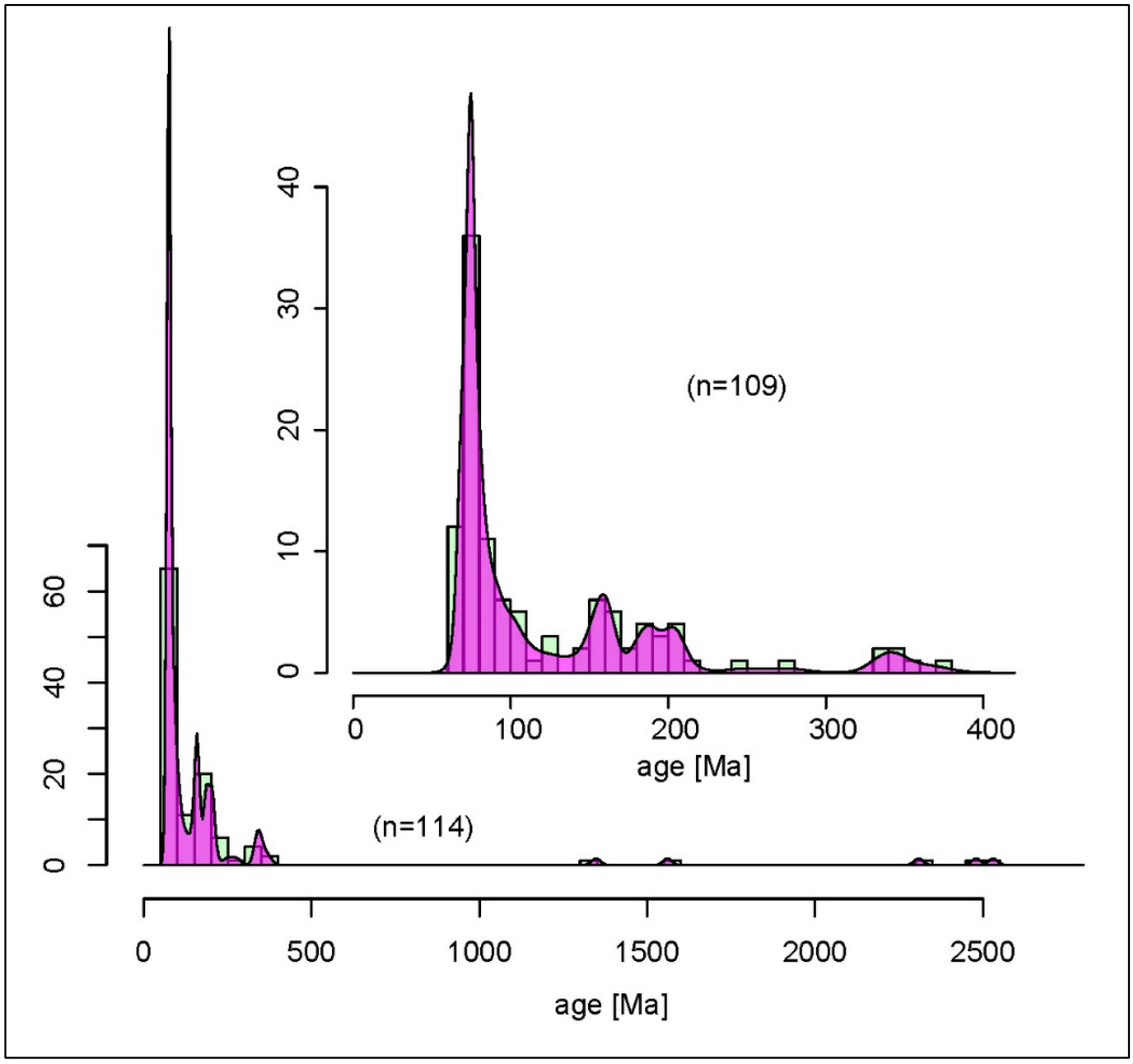

Figure 2. Kernel density estimate of detrital zircon distribution of all dated grains and inset showing distribution from 0 to 400 Ma for sample 12BG300A.

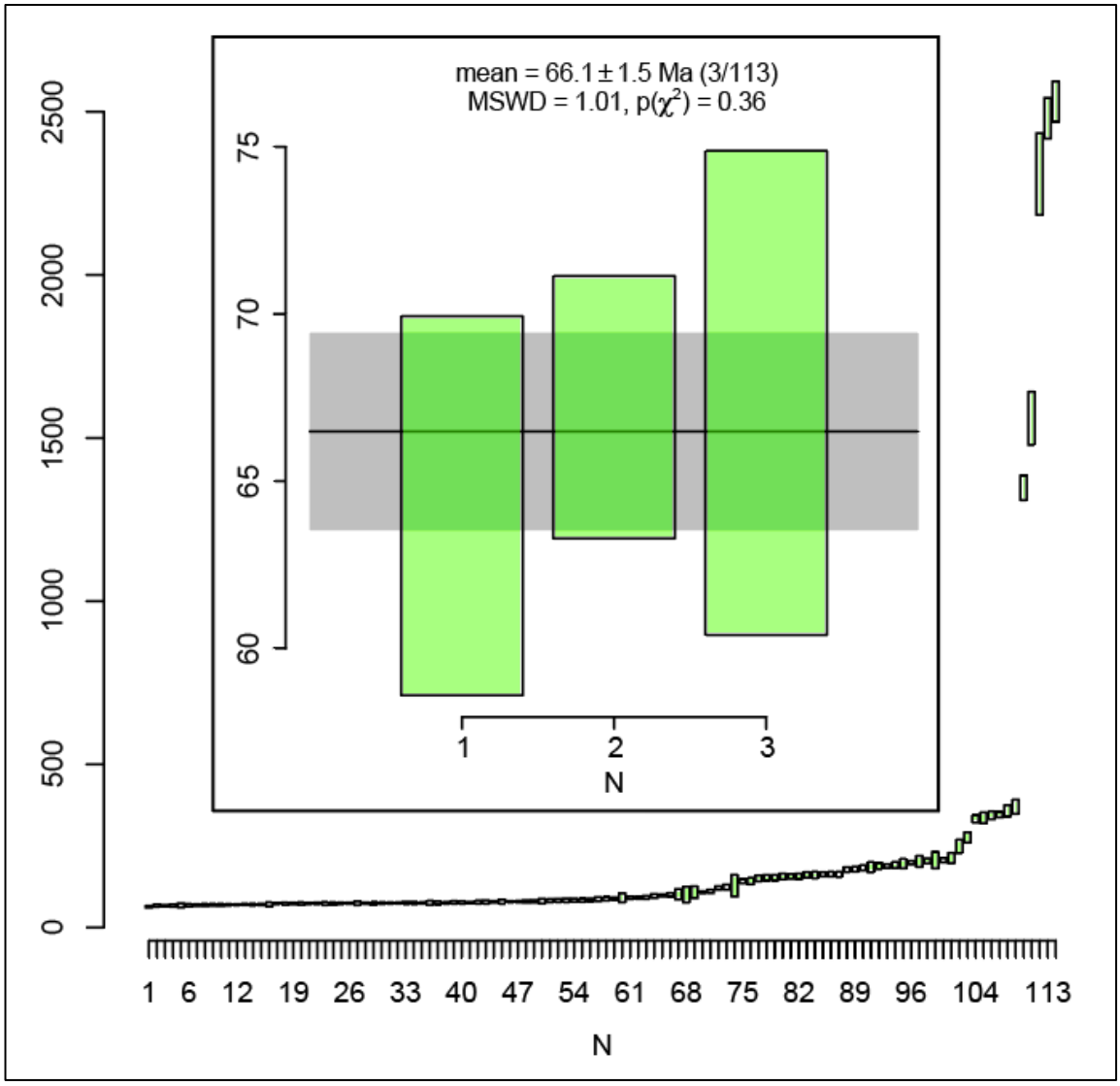

Figure 3. Ranked date plot of entire detrital zircon distribution and inset showing dates calculated for the weighted-mean maximum depositional age for sample 12BG300A. See Bull and others (2024) for a discussion of zircon date selection for this sample.

Sample 12BG303A – Passage Canal Pluton: 38.7±0.9 Ma (n=56, MSWD=2.86, PoF=0.00) Crystallization Age

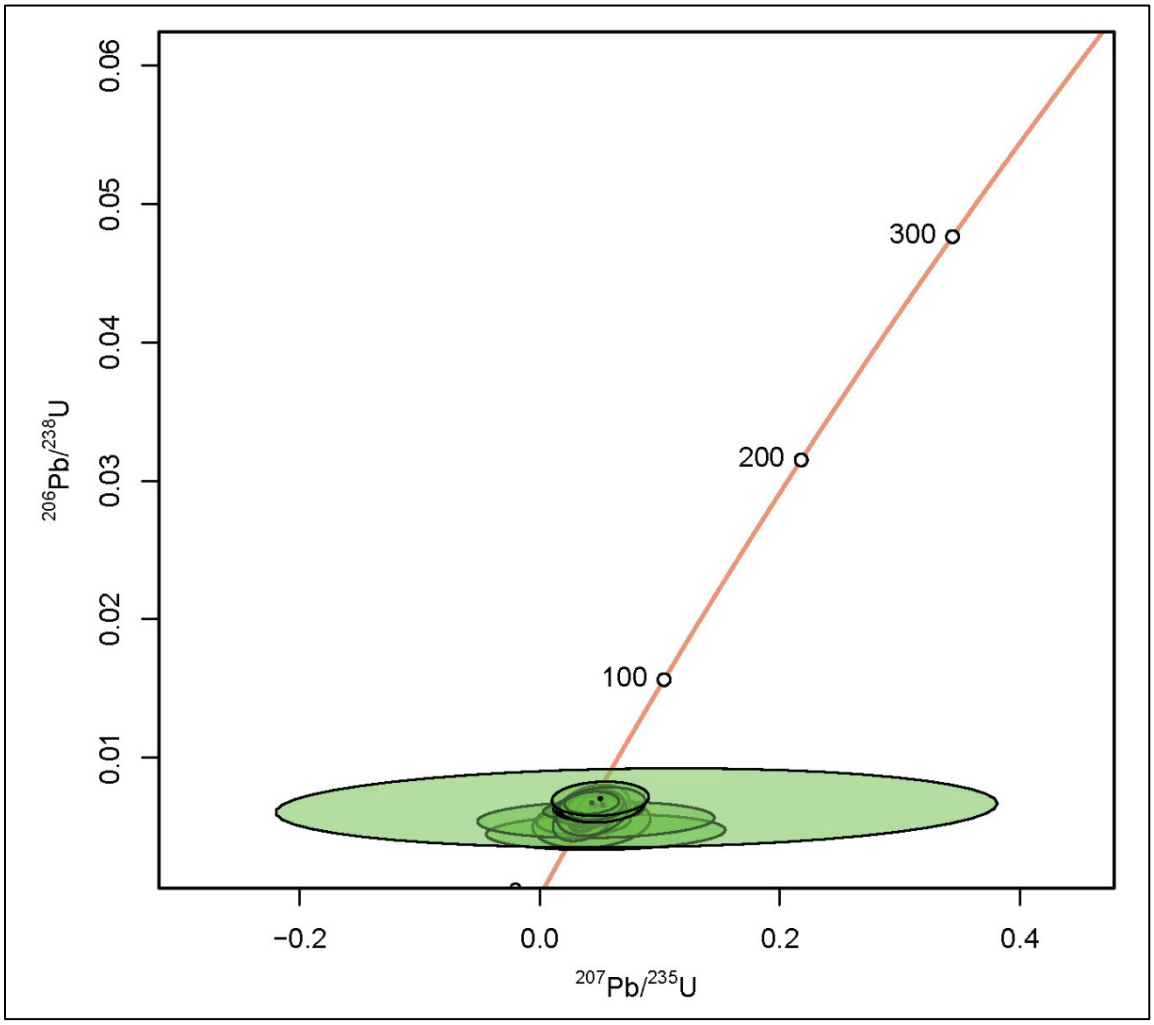

Figure 4. Concordia diagram of individual zircon U-Pb analyses for sample 12BG303A.

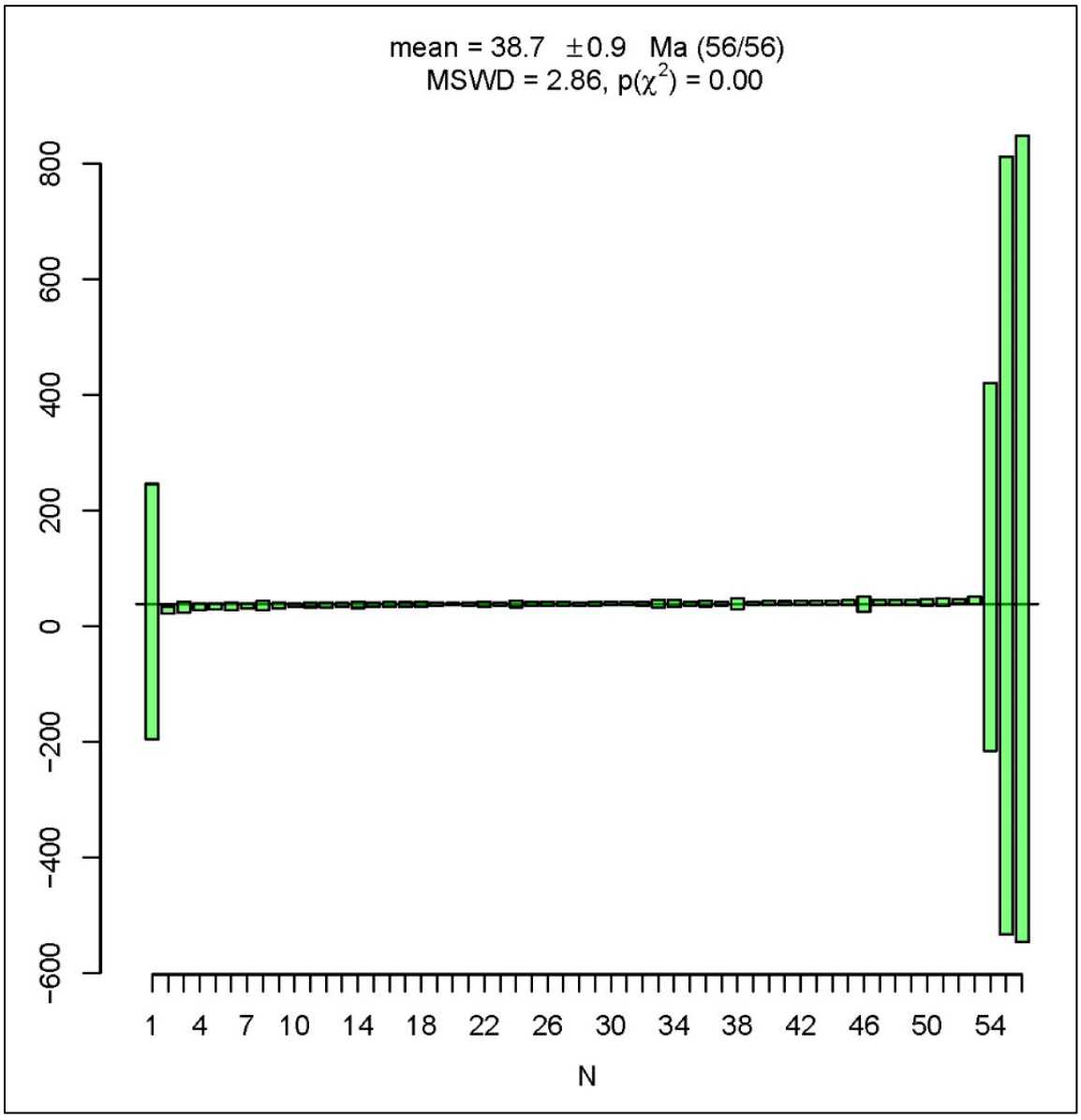

Figure 5. Ranked date plot of entire zircon distribution for sample 12BG303A.

Sample 12BG308A – Billings Pluton: 38.8±0.8 Ma (n=57, MSWD=2.24, PoF=0.00) Crystallization Age

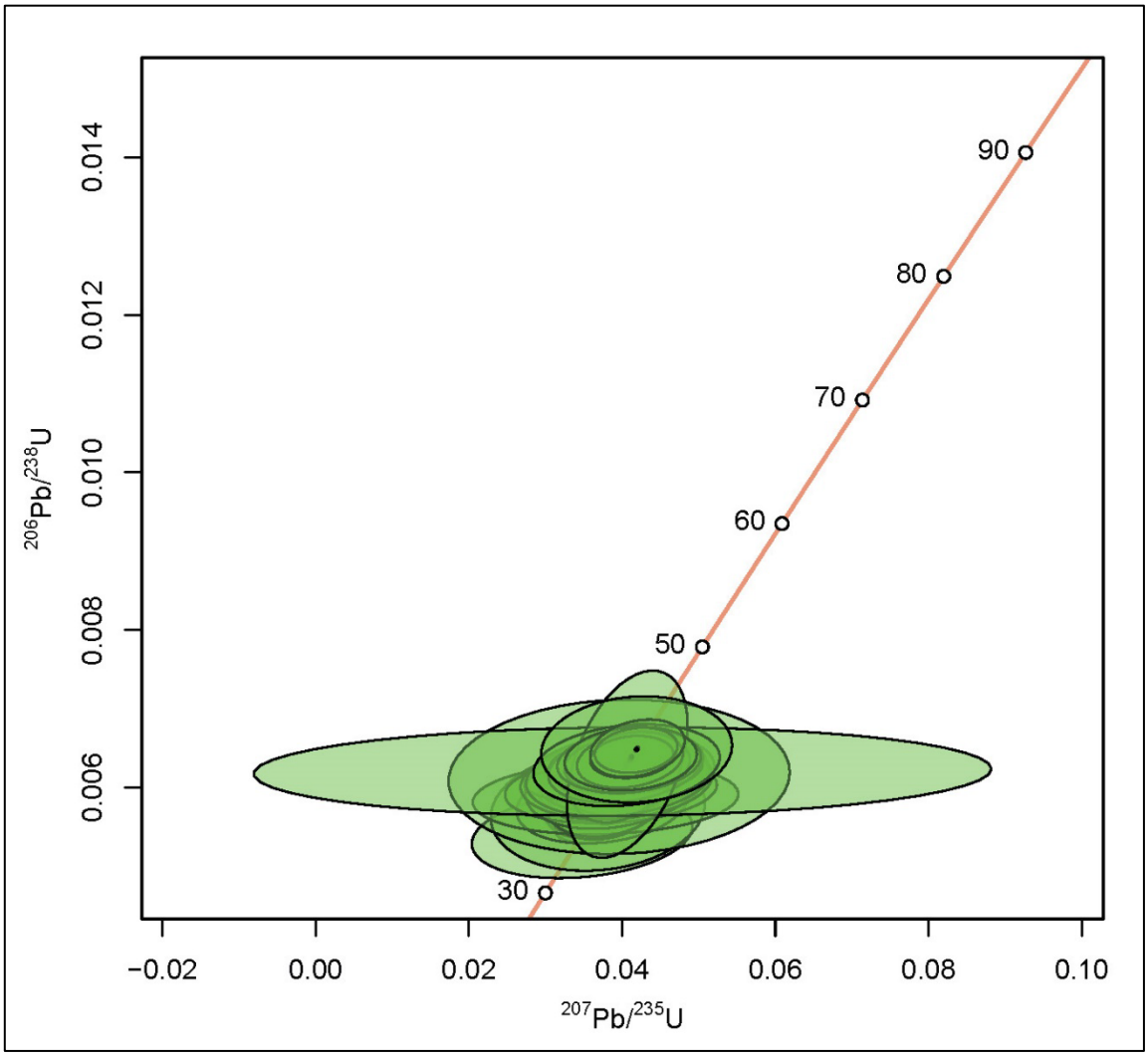

Figure 6. Concordia diagram of individual zircon U-Pb analyses for sample 12BG308A.

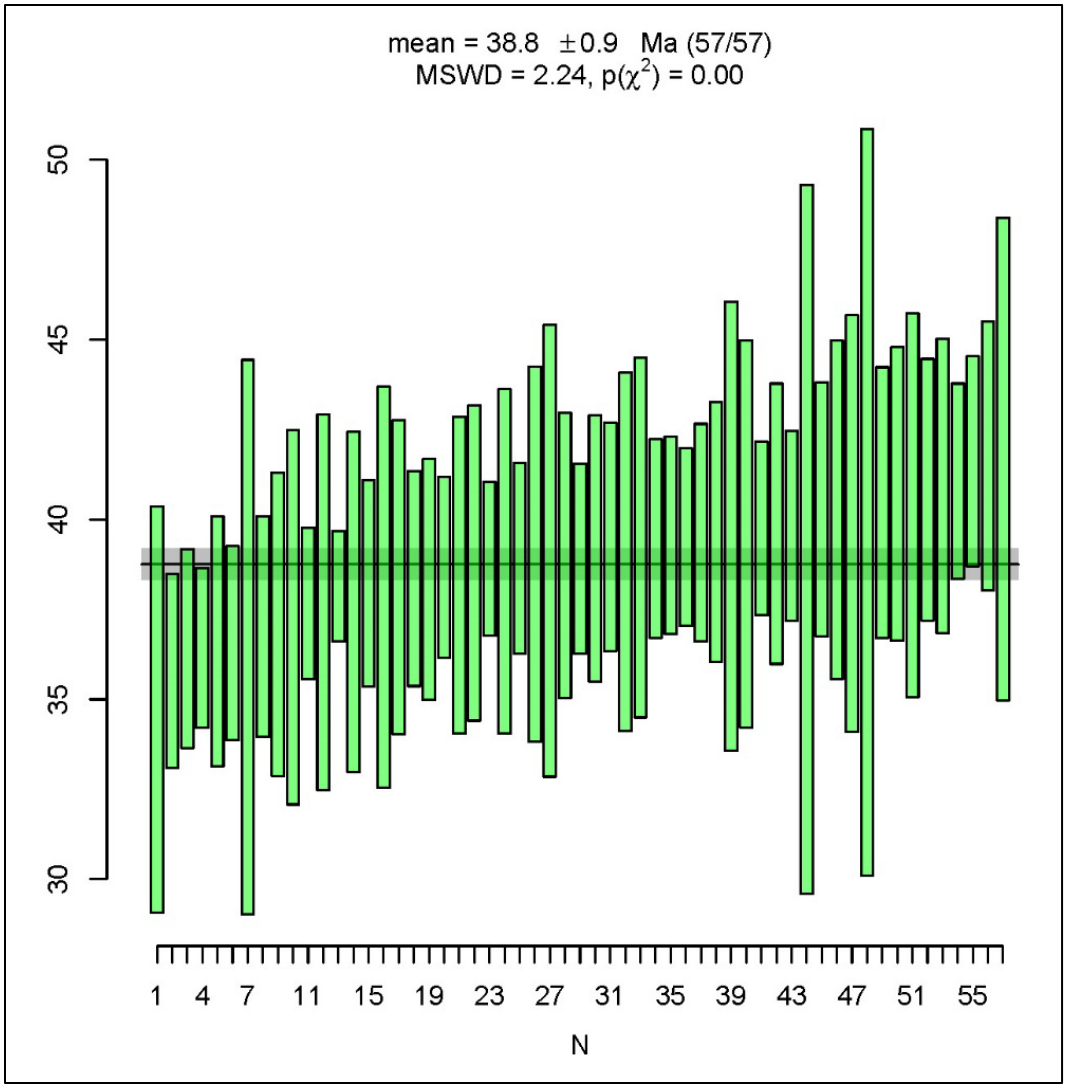

Figure 7. Ranked date plot of entire zircon distribution for sample 12BG308A.

ACKNOWLEDGMENTS

We thank Pathfinder Aviation and pilot Spanky Handley for their exceptional work in difficult circumstances and the people of Whittier for their kindness and generosity. We greatly appreciate the Chugach Alaska Native Corporation and the U.S. Forest Service for their helpfulness and access to their lands during this study.

These analyses were funded by the 2012 U.S. Geological Survey National Cooperative Geologic Mapping Program, award number G12AS00007. The views and conclusions contained in this document are those of the authors and should not be interpreted as representing the opinions or policies of the U.S. Geological Survey. Mention of trade names or commercial products does not constitute their endorsement by the U.S. Geological Survey.

REFERENCES

Barfod, G.H., Krogstad, E.J., Frei, Robert, and Albarède, Francis, 2005, Lu-Hf and PbSL geochronology of apatites from Proterozoic terranes: A first look at Lu-Hf isotopic closure in metamorphic apatite: Geochimica et Cosmochimica Acta, v. 69, no. 7, p. 1,847–1,859.

Black, L.P., and Gulson, B.L., 1978, The age of the Mud Tank carbonatite, Strangways Range, Northern Territory: BMR Journal Australian Geology and Geophysics, v. 3, p. 227–232.

Boyce, J.W., and Hodges, K.V., 2005, U and Th zoning in Cerro de Mercado (Durango, Mexico) fluorapatite: Insights regarding the impact of recoil redistribution of radiogenic ^{4}He on (U-Th)/He thermochronology: Chemical Geology, v. 219, p. 261–274. https://doi.org./10.1016/j.chemgeo.2005.02.007

Bull, K.F., Stevens, D.S.P., Gillis, R.J., Wolken, G.J., and Balazs, M.S., 2024, Geology and geologic hazards in the Whittier area, Southcentral Alaska: Alaska Division of Geological & Geophysical Surveys Preliminary Interpretive Report 2024-4, 18 p., 1 sheet. https://doi.org/10.14509/31426

Campbell, I.H., Ballard, J.R., Palin, J.M., Allen, C.M., and Faunes, Alejandro, 2006, U-Pb zircon geochronology of granitic rocks from the Chuquicamata–El Abra porphyry copper belt of northern Chile: Excimer laser ablation ICP-MS analysis: Economic Geology, v. 101, no. 7, p. 1,327–1,344. https://doi.org/10.2113/gsecongeo.101.7.1327

Charlier, B.L.A., Wilson, C.J.N., Lowenstern, J.B., Blake, S., Van Calsteren, P.W., and Davidson, J.P., 2005, Magma generation at a large, hyperactive silicic volcano (Taupo, New Zealand) revealed by U-Th and U-Pb systematics in zircons: Journal of Petrology, v. 46, no. 1, p. 3–32. https://doi.org/10.1093/petrology/egh060

Coutts, D.S., Matthews, W.A., and Hubbard, S.M., 2019, Assessment of widely used methods to derive depositional ages from detrital zircon populations: Geoscience Frontiers, v. 10, p. 1,421–1,435. https://doi.org/10.1016/j.gsf.2018.11.002

Donelick, R.A., O'Sullivan, P.B., and Donelick, M.B., 2009, A discordia-based method of zircon U-Pb dating from LA-ICP-MS analysis of single spots: Proceedings of the 10th Biennial Meeting of the Society for Geology Applied to Mineral Deposits, Townsville, Australia, August 17–20, 2009, p. 276–278.

Herriott, T.M., Crowley, J.L., Schmitz, M.D., Wartes, M.A., and Gillis, R.J., 2019, Exploring the law of detrital zircon: LA-ICP-MS and CA-TIMS geochronology of Jurassic forearc strata, Cook Inlet, Alaska, USA: Geology, v. 47, no. 11, p.1,044–1,048. https://doi.org/10.1130/G46312.1

Hildreth, Wes, 2001, A critical overview of silicic magmatism, *in* Penrose Conference on Longevity and Dynamics of Rhyolitic Magma Systems, Mammoth, California, June 7–12, 2001, p. 6–12.

Horstwood, M.S., Košler, J., Gehrels, G., Jackson, S.E., McLean, N.M., Paton, C., Pearson, N.J., Sircombe, K., Sylvester, P., Vermeesch, P., and Bowring, J.F., 2016, Community-derived standards for LA-ICP-MS U-(Th-) Pb geochronology–Uncertainty propagation, age interpretation and data reporting: Geostandards and Geoanalytical Research, v. 40, no. 3, p. 311–332.

Kryza, R., Crowley, Q.G., Larionov, Alexander, Pin, Christian, Oberc-Dziedzic, Teresa, and Mochnacka, Ksenia, 2012, Chemical abrasion applied to SHRIMP zircon geochronology: An example from the Variscan Karkonosze Granite (Sudetes, SW Poland): Gondwana Research, v. 21, no. 4, p. 757–767. https://doi.org/10.1016/j.gr.2011.07.007

Kuiper, K.F., Deino, Alan, Hilgen, P.J., Krijgsman, Wout, Renne, P.R., and Wijbrans, J.R., 2008, Synchronizing rock clocks of Earth history: Science, v. 320, p. 500–504. https://doi.org/10.1126/science.1154339

Lanphere, M.A., and Baadsraard, H., 2001, Precise K-Ar, $^{40}Ar/^{39}Ar$, Rb-Sr and UPb mineral ages from the 27.5 Ma Fish Canyon Tuff reference standard: Chemical Geology, v. 175, p. 653–671.

McDowell, F.W., McIntosh, W.C., and Farley, K.A., 2005, A precise $^{40}Ar/^{39}Ar$ reference age for the Durango apatite (U-Th)/He and fission-track dating standard: Chemical Geology, v. 214, no. 3–4, p. 249–263.

Miller, J.S., Matzel, J.E.P., Miller, C.F., Burgess, S.D., and Miller, R.B., 2007, Zircon growth and recycling during the assembly of large, composite arc plutons: Journal of Volcanology and Geothermal Research, v. 167, no. 1–4, p. 282–299. https://doi.org/10.1016/j.jvolgeores.2007.04.019

Paces, J.B., and Miller, J.D., 1993, Precise UPb ages of Duluth Complex and related mafic intrusions, northeastern Minnesota: Geochronological insights to physical, petrogenic, paleomagnetic, and tectonomagmatic processes associated with the 1.1 Ga Midcontinent Rift System: Journal of Geophysical Research, v. 98, no. B8, p. 13,997–14,013.

Renne, P.R., Swisher, C.C., Deino, A.L., Karner, D.B., Owens, T.L., and DePaolo, D.J., 1998, Intercalibration of standards, absolute ages and uncertainties in $^{40}Ar/^{39}Ar$ dating: Chemical Geology, v. 45, p. 117–152.

Roden, M.K., Parrish, R.R., and Miller, D.S., 1990, The absolute age of the Eifelian Tioga ash bed: Journal of Geology, v. 98, p. 282–285.

Savitzky, Abraham, and Golay, M.J., 1964, Smoothing and differentiation of data by simplified least squares procedures: Analytical Chemistry, v. 36, no. 8, p. 1,627–1,639.

Schoene, Blair, and Bowring, S.A., 2006, UPb systematic of the McClure Mountain syenite: thermochronological constraints on the age of the $^{40}Ar/^{39}Ar$ standard MMhb: Contributions to Mineralogy and Petrology, v. 151, p. 615–630. https://doi.org/10.1007/s00410-006-0077-4

Siegel, Coralie, Bryan, S.E., Allen, C.M., and Gust, D.A., 2018, Use and abuse of zircon-based thermometers: A critical review and a recommended approach to identify antecrystic zircons: Earth-Science Reviews, v. 176, p. 87–116. https://doi.org/10.1016/j.earscire.2017.08.011

Spencer, C.J., Kirkland, C.L., and Taylor, R.J., 2016, Strategies towards statistically robust interpretations of in situ U–Pb zircon geochronology: Geoscience Frontiers, v. 7, no. 4, p. 581–589. https://doi.org/10.1016/j.gsf.2015.11.006

Vermeesch, Pieter, 2018, IsoplotR: a free and open toolbox for geochronology: Geoscience Frontiers, v. 9, p. 1,479–1,493. doi.org/10.1016/j.gsf.2018.04.001

Weidenbeck, Michael, Alle, Priyanka, Corfu, F., Griffin, W.L., Meier, M., Oberli, F., von Quandt, Albrecht, Roddick, J.C., and Speigel, W., 1995, Three natural zircon standards for U-Th-Pb, Lu-Hf, trace-element and REE analyses: Geostandards Newsletter, v. 19, p. 1–23.

Yuan, H.-L., Gao, Shan, Dai, M.-N., Zong, C.-L., Günther, Detlef, Fontaine, G.H., Liu, X.-M., and Diwu, ChunRong, 2008, Simultaneous determinations of UPb age, Hf isotopes and trace element compositions of zircon by excimer laser-ablation quadrapole and multiple-collector ICP-MS: Chemical Geology, v. 247, p. 100–118.